

Tunable and frequency-stabilized diode laser with a Doppler-free two-photon Zeeman lock

Stanislav Balushev, Nir Friedman, Lev Khaykovich, Dina Carasso, Ben Johns, and Nir Davidson

We describe frequency locking of a diode laser to a two-photon transition of rubidium using the Zeeman modulation technique. We locked and tuned the laser frequency by modulating and shifting the two-photon transition frequency with ac and dc magnetic fields. We achieved a linewidth of 500 kHz and continuous tunability over 280 MHz with no laser frequency modulation. © 2000 Optical Society of America

OCIS codes: 020.7490, 140.2020, 300.6260

1. Introduction

Diode lasers serve as a common light source for many areas in optical communication and spectroscopy because of their high reliability, high efficiency, good power stability, and large frequency tunability.¹ However, even single-mode diode lasers typically have a >10-MHz free-running linewidth, which is too large for many applications. Narrow (<1-MHz) linewidth and continuous tunability are obtained, for example, by use of an external cavity with a diffraction grating.² The grating reflects its first-order diffracted beam back to the diode laser in a so-called Littrow configuration to set the desired frequency.

For high-resolution spectroscopy experiments, long-term stability of the laser frequency might be required, which is best ensured by frequency locking to atomic or molecular absorption lines. Saturation-absorption techniques typically yield a Doppler-free linewidth of a few megahertz at which the laser is locked.³ Moreover, continuous tunability of the lock frequency enables a combination of source tunability and long-term stability without the need for external frequency shifters, such as acousto-optic modulators. To generate a tunable laser line with such properties,

a number of methods were developed, including frequency offset locking⁴ and side locking⁵ that enable one to lock the laser frequency at a controlled offset from an atomic line.

An alternative approach is to lock the laser frequency always to the center of the atomic line and to modulate the atomic line itself by application of an alternating magnetic field.⁶ The modulated signal can then be detected by use of a lock-in amplifier to generate a dispersive signal, which is highly advantageous for stable frequency locking on a zero crossing feature at the absorption line center.⁷ Other modulation schemes, which are used to produce a dispersive lock signal, usually involve modulation of the laser frequency,⁸ which is a disadvantage for some applications. Moreover, by adding a dc magnetic field the atomic line can also be Zeeman shifted, hence tuning the frequency of the locked laser. Since the Zeeman shift can be much larger than the linewidth, this approach enables a relatively large tuning range while maintaining a narrow reference line and thus a suppression of most line-offset drifts.⁹ Compared with other frequency locking⁸ and tuning^{4,5} schemes, this method does not require expensive optical and electronic components and does not involve laser frequency modulation; it is a simple combination of frequency modulation (for the locking) and tuning.

Here we report on a new scheme that locks the diode-laser frequency to a Doppler-free two-photon atomic line ($5\ ^2S_{1/2} \rightarrow 5\ ^2D_{5/2}$ in ^{87}Rb and ^{85}Rb). The line is Zeeman modulated by an axial ac magnetic field and Zeeman shifted by an additional axial dc magnetic field to obtain a tunable dispersive signal for the lock. Our scheme yields several important

When this research was performed, the authors were with the Department of Physics of Complex Systems, Weizmann Institute of Science, Rehovot 76100, Israel. S. Balushev is now with the Institute of Applied Physics, Technical University of Sofia, 1780 Sofia, Bulgaria. The e-mail address for N. Davidson is fedavid@wis.weizmann.ac.il.

Received 23 February 2000; revised manuscript received 30 June 2000.

0003-6935/00/274970-05\$15.00/0

© 2000 Optical Society of America

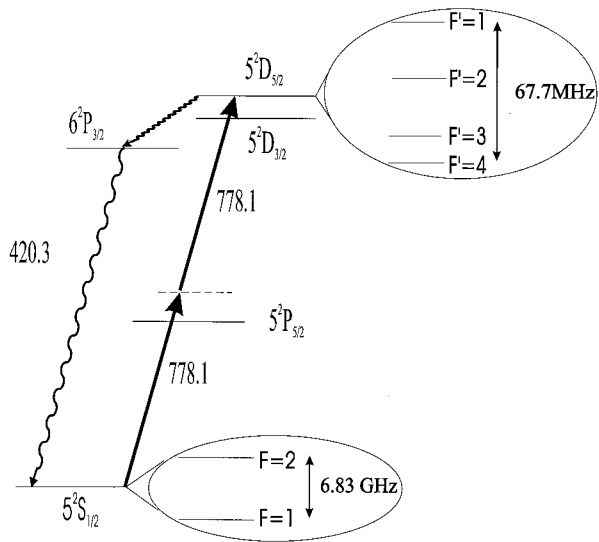


Fig. 1. Schematic energy diagram of the ^{87}Rb two-photon transition.

advantages: (i) Neither modulation of the laser frequency nor use of external frequency modulators is required for locking. (ii) The large Lande g factor of the two-photon excited state enables larger frequency tunability, compared with one-photon locking schemes with identical strength of the magnetic field. (iii) Because of its inherent nonlinearity, most of the two-photon absorption occurs in a small volume that surrounds the focus of the laser beams; hence relatively large and extremely uniform magnetic fields are readily obtained. (iv) This locking scheme enables access to many other frequencies and atomic lines that are inaccessible with one-photon locking schemes and is particularly useful for two-photon spectroscopy experiments.

2. Experiment and Results

The relevant energy levels for ^{87}Rb are shown in Fig. 1. The ground state of ^{87}Rb is split by 6.835 GHz into two hyperfine components with $F = 2$ and $F = 1$. This split is larger than the 670-MHz two-photon Doppler width for the system at a temperature of 430 K. The upper $5^2D_{5/2}$ level has four F sublevels with a hyperfine split of $\sim 15\text{--}30$ MHz.¹⁰ For the other isotope studied, ^{85}Rb , the levels are similar except that the splitting of the hyperfine levels is approximately 2–3 times smaller.

The main problem with two-photon frequency lock compared with the one-photon lock is the much lower signal that is obtained when a relatively weak (a few milliwatts) cw laser is used. In the realization of our scheme this difficulty was reduced for several reasons. First, we used the two-photon transition $5S$ to $5D$ in rubidium whose 778.1-nm wavelength is only ~ 2 nm detuned from the strong one-photon transition, which largely enhances the transition cross section. Second, by focusing the laser beam, we obtained relatively high intensities in the focal region even for low laser power. Third, we used two coun-

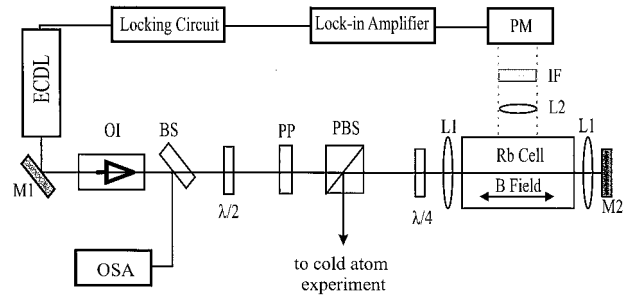


Fig. 2. Experimental setup: ECDL, external cavity diode laser; M1, M2, mirrors; L1, L2, lenses; IO, optical isolator; BS, beam splitter; OSA, optical spectrum analyzer; PP, prism pair; PBS, polarizing beam splitter; IF, interference filter; PM, photomultiplier.

terpropagating beams with an inverse Doppler shift so that all the atoms contributed to a Doppler-free signal.¹¹ This yields an ~ 100 -fold enhancement compared with Doppler-free spectroscopy for one-photon transitions in which only a very narrow velocity class of atoms (usually near $v = 0$) contributes to the Doppler-free signal.¹² Finally, we used the fluorescence signal rather than the absorption signal and hence obtained a good ($>300:1$) signal-to-noise ratio even though our two-photon absorption is only $\sim 0.1\%$.

The experimental setup for the two-photon lock is shown in Fig. 2. We used a homemade external cavity diode laser in a Littrow configuration.¹³ The laser output power was ~ 20 mW at a wavelength of 778.1 nm, of which we used typically 3–10 mW for the frequency lock (the remaining power was sent to a dark optical trap to perform two-photon spectroscopy of cold rubidium atoms.¹⁴) Stabilizing the heat sink temperature to ~ 1 mK and the injection current to ~ 1 μA ensured an instantaneous laser linewidth of ~ 500 kHz and thermal drifts less than 1 MHz/s.

The beam passed through two optical isolators in series, each with 40-dB isolation (to avoid undesired optical feedback) and a 2:1 anamorphic prism pair to reduce its ellipticity. It was then focused into a vapor cell (which contained a natural rubidium mixture) to a waist of 100 μm and retroreflected with a cat's-eye configuration. This waist size was chosen to reduce the time-of-flight broadening and still obtain a reasonable signal-to-noise ratio. Narrower waists yielded larger signals, but also an observable time-of-flight broadening and larger sensitivity to long-term drifts and fluctuations of the relative beam alignment. The focus of the two counterpropagating beams was carefully adjusted to overlap in all three dimensions. Polarization of the laser beams was controlled with a polarizer and a quarter-wave plate to produce linear, σ^+ or σ^- polarization for both beams. We obtained a rubidium pressure of a few millitorr by heating the vapor cell to a temperature of 430 K with heating coils. Two solenoids for Zeeman shift and modulation generated the axial dc magnetic field and the axial ac magnetic field at the cell center, respectively. The fluorescence at 420.3 nm arising

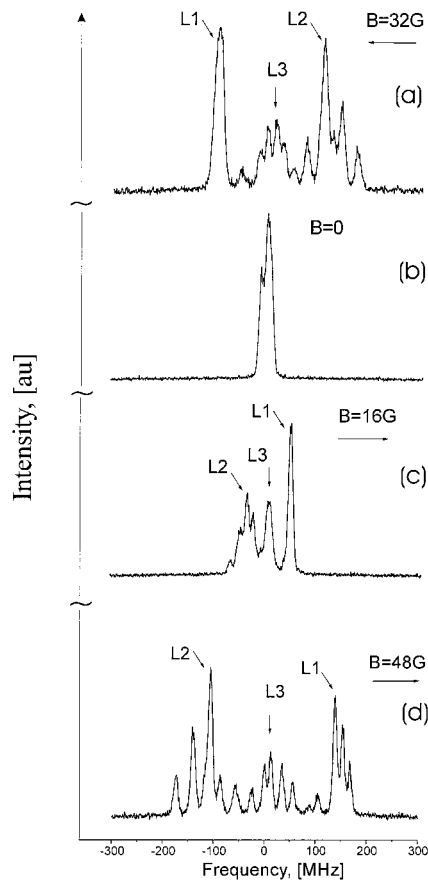


Fig. 3. Zeeman-shifted two-photon signal at linear polarization and various values of the magnetic field magnitude for the transition $5^2S_{1/2}, F_g = 1 \rightarrow 5^2D_{5/2}, F_e = 1-3$ in ^{87}Rb . The intensity axis was rescaled for clarity.

from the $5^2D_{5/2} \rightarrow 6^2P_{3/2} \rightarrow 5^2S_{1/2}$ cascade decay (see Fig. 1) was imaged with an $F/1.5$ lens to a photomultiplier tube covered with a narrow horizontal slit (passing light only from the elongated focal region) and a 420-nm interference filter. The final alignment of the beams and the slit was performed to maximize the two-photon fluorescence signal and to reduce background. The total fluorescence power detected by the photomultiplier was $\sim 1 \mu\text{W}$. An ~ 200 times weaker Doppler-broadened signal was also observed because of two-photon absorption from each beam separately.

The measured two-photon absorption spectra depended on the polarization of the laser beams and on the magnitude and direction of the applied dc magnetic field. The 420.3-nm fluorescence signal obtained for different magnitude and direction of the dc magnetic field and for a linear polarization of both laser beams for the $5^2S_{1/2}, F_g = 1 \rightarrow 5^2D_{5/2}, F_e = 1-3$ in ^{87}Rb atoms is shown in Fig. 3. Similar data were also obtained for the transition $5^2S_{1/2}, F_g = 2 \rightarrow 5^2D_{5/2}$ and for the two transitions in ^{85}Rb atoms: $5^2S_{1/2}, F_g = 2 \rightarrow 5^2D_{5/2}$ and $5^2S_{1/2}, F_g = 3 \rightarrow 5^2D_{5/2}$. When the polarization is linear, the spectrum contains components that correspond to absorption of photons with (σ^+, σ^+) , (σ^-, σ^-) , and (σ^-, σ^+) polar-

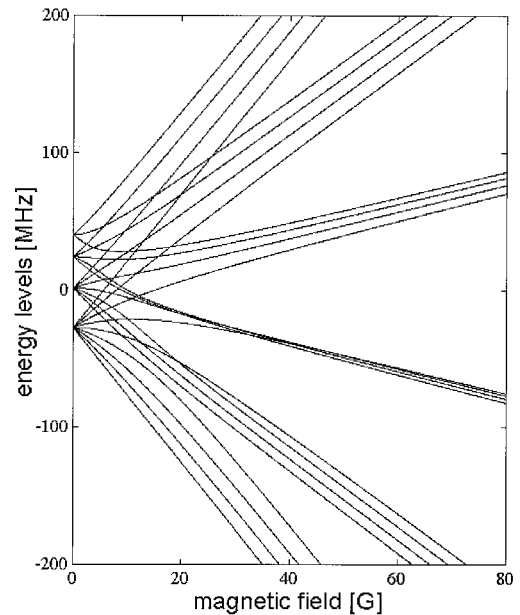


Fig. 4. Calculated Zeeman-shifted energy levels of the $5^2D_{5/2}$ excited state of the ^{87}Rb atom.

izations from the forward- and backward-propagating beam, respectively. The cluster of peaks labeled L1 in Fig. 3 corresponds to (σ^-, σ^-) polarization. It shifts toward higher optical frequencies for one direction of the increasing magnetic field and toward lower frequencies when the magnetic field is reversed. The cluster of peaks labeled L2 corresponds to (σ^+, σ^+) polarization and, accordingly, shifts the opposite way. It can also be seen that, for different circular polarization, the Zeeman shift differs; see Figs. 3(a) and 3(d). The L3 cluster in the middle corresponds to (σ^-, σ^+) polarization. Note that the different peaks in each cluster become separate only above some magnetic field that induces a sufficient Zeeman shift. However, as described below, locking and tuning of the laser were possible over the whole range. The widths of the resolved two-photon hyperfine lines were 7 MHz (FWHM), caused partly by the time-of-flight broadening (~ 4 MHz) and partly by pressure broadening as a result of residual buffer gas contamination in the cell.

In general, to calculate the Zeeman shift of the excited-state levels, one must diagonalize the hyperfine structure Hamiltonian¹⁵ expressed in matrix form on the basis of magnetic quantum numbers m_I and m_J . The calculated energy levels as a function of magnetic field for the $5^2D_{5/2}$ excited state of the ^{87}Rb atom are shown in Fig. 4. The dc magnetic field that was used throughout our experiment was less than 70 G. For this field strength, the hyperfine I - J coupling of the $5^2S_{1/2}$ ground state does not significantly break down and the appropriate Zeeman shift of the ground-state energy levels changes linearly with the magnetic field. Thus, the energy shifts of the (F, m_F) components of the ground state were found to be of the order of 50 MHz. In contrast,

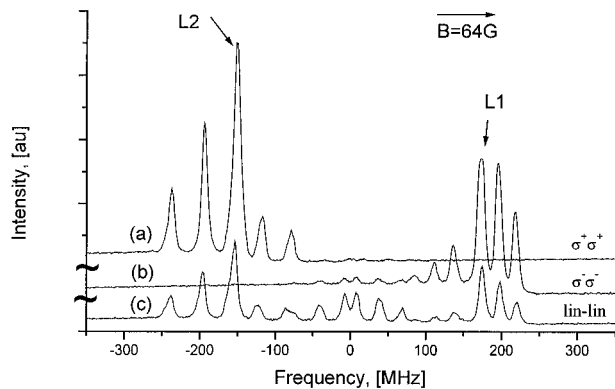


Fig. 5. Zeeman-shifted two-photon signal for different polarizations and a fixed magnitude of the dc magnetic field for the transition $5\ ^2S_{1/2}, F_g = 1 \rightarrow 5\ ^2D_{5/2}, F_e = 1-3$ in ^{87}Rb . The curves were shifted vertically for clarity.

for such a field, Zeeman splitting of the upper $5D$ state is much larger than the hyperfine splitting in a zero magnetic field,¹⁶ thus the Zeeman–Hamiltonian matrix diagonalization is needed. The frequency position of the measured lines agrees well with the calculated level shifts. For a relatively small magnetic field strength (<70 G) it is seen that the Zeeman shift for (σ^+, σ^+) and (σ^-, σ^-) polarizations differs significantly, which is also observed in the experimental data shown in Figs. 3(a), 3(c), and 3(d). It can also be seen that, because of the higher Lande g factor of this level, the Zeeman shifts are larger than for the ground state and hence a larger tunability range was achieved.

Figure 5 presents the measured fluorescence signal for different polarizations and a fixed magnitude of the magnetic field. In the case of linear–linear polarization, the relative intensity of the resolved peaks drops significantly compared with the intensity of circular $[(\sigma^+, \sigma^+) \text{ or } (\sigma^-, \sigma^-)]$ polarization, but the frequency position does not change. An advantage of locking the laser with circular polarization is the 3–4 times better signal-to-noise ratio of the fluorescence signal.

We Zeeman modulated the rubidium resonance frequency by applying a 0.2-A ac current to the solenoid that corresponds to an ~ 1.5 -MHz frequency excursion. The lock-in amplifier produced a derivative signal, which was used as an error signal for the locking circuit. The low-frequency part of the error signal was fed to a piezoelectric transducer that controlled the external cavity of the laser and the high-frequency part was used for current feedback to the diode laser. The instantaneous rms laser linewidth during locking the laser was ~ 500 kHz, comparable with that of an unlocked line. Stable locking was possible for many hours with high durability to mechanical and acoustic noise.

For small dc magnetic fields, the hyperfine structure of the $5\ ^2D_{5/2}$ level was unresolved, yielding a complicated shape of the corresponding derivative signals, as shown, for example, in Fig. 6 for $B = 0$.

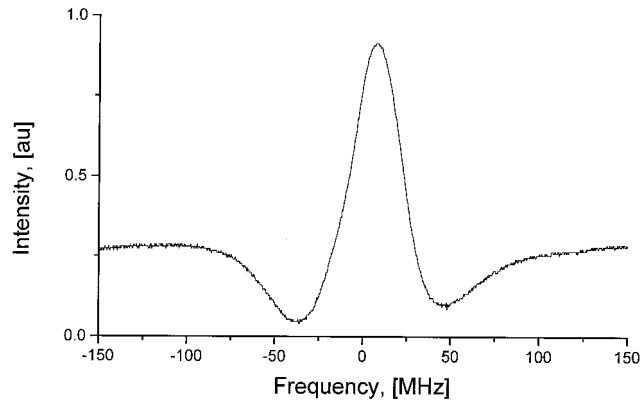


Fig. 6. Derivative signal at zero dc magnetic field for the transition $5\ ^2S_{1/2}, F_g = 1 \rightarrow 5\ ^2D_{5/2}, F_e = 1-3$ in ^{87}Rb .

Even with the asymmetry and the higher width of the derivative signal of this unresolved cluster of lines, stable locking was still possible. This allowed us to maintain continuous locking even when the magnetic field crossed zero. We tuned the lock point of the laser by varying the dc magnetic field. We measured the frequency shift by comparing the spectrum with that of a zero dc magnetic field. For the L1 cluster (σ^-, σ^-) polarization (see Fig. 3), good signals for continuous locking were obtained over a range exceeding ± 140 MHz from the zero field resonance by applying a dc magnetic field of ± 50 G. Figure 7 displays the lock point detuning of the L1 zero crossing point for ^{87}Rb as a function of the dc magnetic field. As seen, the shift is approximately linear for the entire frequency range in agreement with the calculations of Fig. 4. For higher dc magnetic fields (>50 G) the hyperfine spectra obtained with (σ^+, σ^+) polarization is well resolved [see Figs. 3(d) and 5(a)] and continuous locking on the L2 line was also possible with an even higher signal-to-noise ratio than for the L1 line but with a smaller tuning range. Finally, similar results were also obtained for the $5\ ^2S_{1/2}, F_g = 2 \rightarrow 5\ ^2D_{5/2}$ transition in ^{87}Rb and for the

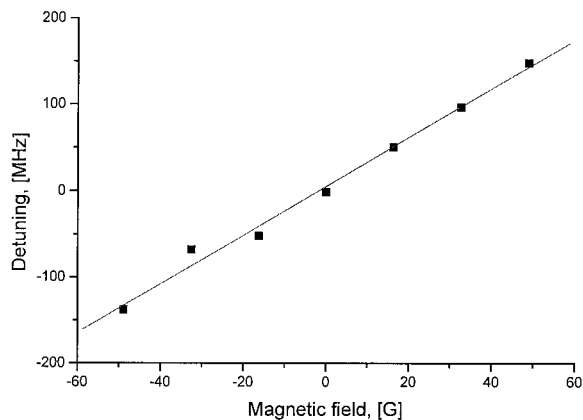


Fig. 7. Lock point detuning as a function of magnetic field magnitude for (σ^-, σ^-) polarization. The line is a linear fit ($\Delta F = \alpha B$) to the experimental data with $\alpha = 2.82$ MHz/G.

two transitions in ^{85}Rb atoms: $5\ ^2S_{1/2}, F_g = 2 \rightarrow 5\ ^2D_{5/2}$ and $5\ ^2S_{1/2}, F_g = 3 \rightarrow 5\ ^2D_{5/2}$.

3. Conclusions

In conclusion, we have demonstrated a simple scheme for locking diode lasers on a Doppler-free two-photon absorption line in rubidium atoms, based on Zeeman modulation and tuning of the atomic line with a combination of ac and dc magnetic fields. We achieved a stable lock with a laser linewidth of 500 kHz and continuous locking point tunability of 280 MHz, without laser frequency modulation. The large Lande g factor of the two-photon excited state enables larger frequency tunability compared with one-photon locking schemes with identical magnetic field strength. Combining the advantages of such a two-photon locking scheme and available acousto-optic frequency shifters enables spectroscopic access to many other atomic lines that are otherwise inaccessible for high-precision spectroscopy with one-photon locking schemes. This was recently demonstrated by performing a two-photon spectroscopy in cold rubidium atoms inside a dark optical trap.¹⁴

References

1. C. Wieman and L. Hollberg, "Using diode lasers for atomic physics," *Rev. Sci. Instrum.* **62**, 1–20 (1991).
2. K. MacAdam, A. Steinbach, and C. Wieman, "A narrow-band tunable diode-laser system with grating feedback, and a saturated absorption spectrometer for Cs and Rb," *Am. J. Phys.* **60**, 1098–1111 (1992).
3. W. Demtroder, *Laser Spectroscopy* (Springer-Verlag, New York, 1996), Chap. 4.
4. J. Maki, N. Campbell, C. Grande, R. Knorpp, and D. McIntyre, "Stabilized diode-laser system with grating feedback and frequency-offset locking," *Opt. Commun.* **102**, 251–256 (1993).
5. J. Hall, M. Long-Sheng, and G. Kramer, "Principles of optical phase-locking: application to internal mirror He–Ne lasers phase-locked via fast control of the discharge current," *IEEE J. Quantum Electron.* **QE-23**, 427–433 (1987).
6. R. Valenzuela, L. Cimini, R. Wilson, D. Reichmann, and A. Grot, "Frequency stabilization of AlGaAs lasers to absorption-spectrum of rubidium using Zeeman effect," *Electron. Lett.* **24**, 725–726 (1988); A. Weis and S. Derler, "Doppler modulation and Zeeman modulation: laser frequency stabilization without direct frequency modulation," *Appl. Opt.* **27**, 2662–2665 (1988).
7. J. Kawakami, M. Kourogi, and M. Ohtsu, "Computer-controlled narrow-linewidth and frequency-stable AlGaAs laser system with unmodulated output," *Jpn. J. Appl. Phys.* **33**, 1623–1627 (1994).
8. See, e.g., W. D. Lee, J. C. Campbell, R. J. Brecha, and H. J. Kimble, "Frequency stabilization of an external-cavity diode laser," *Appl. Phys. Lett.* **57**, 2181–2183 (1990).
9. T. Dinneen, C. Wallace, and P. Gould, "Narrow linewidth, highly stable, tunable diode-laser system," *Opt. Commun.* **92**, 277–282 (1992).
10. F. Nez, F. Biraben, R. Felder, and Y. Millerioux, "Optical frequency determination of the hyperfine components of the $5S_{1/2} - 5D_{3/2}$ 2-photon transitions in rubidium," *Opt. Commun.* **102**, 432–438 (1993).
11. V. Vuletic, V. Sautenkov, C. Zimmermann, and T. Hansch, "Measurement of cesium resonance line self-broadening and shift with Doppler-free selective reflection spectroscopy," *Opt. Commun.* **99**, 185–190 (1993).
12. S. Svanberg, *Atomic and Molecular Spectroscopy* (Springer-Verlag, Berlin, 1991), Chap. 3.
13. R. Ludeke and E. Harris, "Tunable GaAs laser in an external dispersive cavity," *Appl. Phys. Lett.* **20**, 499–500 (1972).
14. L. Khaykovich, N. Friedman, S. Balushev, D. Fathi, and N. Davidson, "Ultrasensitive two-photon spectroscopy in a dark optical trap, based on long spin-relaxation times," *Europhys. Lett.* **50**, 454–459 (2000).
15. C. Townes and A. Schawlow, *Microwave Spectroscopy* (Dover, New York, 1975), Chap. 5.
16. D. Fulton, R. Mosely, S. Shephard, B. Sinclair, and M. Dunn, "Effects of Zeeman splitting on electromagnetically-induced transparency," *Opt. Commun.* **116**, 231–239 (1995).